

Micron-gap rhe-optics with parallel plates

Ali Dhinojwala and Steve Granick

Department of Material Science and Engineering, University of Illinois, Urbana, Illinois 61801

(Received 19 May 1997; accepted 18 August 1997)

Solid planar plates with area up to several square centimeters can be made parallel at controllable separations from ca. 0.1 (if airborne dust is eliminated) to $>500 \mu\text{m}$. Apart from dust and surface roughness, which set the lower bound of plate-plate separation, there is no other fundamental constraint on the type of surface (metallic or dielectric; opaque or translucent) that can be studied. When conducting plates are employed, it is possible to apply an electric field in the direction normal to the plates and observe the competition between shear fields and electric fields in orthogonal directions. The large surface area should afford sufficient quantity of sample to make possible various spectroscopic and scattering experiments (especially infrared and dielectric spectroscopy in the direction normal to the plates, and x-ray and neutron reflectivity). © 1997 American Institute of Physics. [S0021-9606(97)50144-9]

I. INTRODUCTION

Meso-scale dimensions present a twilight zone between nanoscopic and bulk behavior. We are concerned here principally with fluids. Flow comprises the classical interest of rheology, generations of research having led to sophisticated understanding here, provided that the sample size is macroscopic.¹ New instruments have also been devised recently to measure the rheological or frictional responses of nanoscopic-sized films, films whose thickness is comparable to those of molecules.²⁻⁵ However, molecular organization at intermediate length scales dominates flow phenomena when self-assembled structures on larger length scales than the size of a single molecule come into play. Examples include phase separation processes, the flow of biological cells and colloidal-sized particles in suspension, questions of wall slip in polymers, and surfactant and block polymer microstructures.

We describe here a device to perform rheo-optical experiments at these intermediate length scales. In designing this parallel-plate apparatus, our goals were the following:

(1) There should be no fundamental limitation on the type of confining solid surface (metallic or dielectric; opaque or translucent) that can be employed.

(2) The plate spacing should be controllable and it should be possible to characterize shear viscoelastic response of the sample fluid at all plate spacings.

(3) Direct spectroscopic experiments (e.g., infrared, optical, dielectric) should be possible during the course of shear. The apparatus should also be compact enough to be portable to beam lines (e.g., x-ray and neutron sources) for reflectivity experiments.

(4) The surface area should be adjustable from millimeters on a side for spectroscopic measurements, to centimeters on a side for x-ray and reflectivity measurements.

The motive to use parallel plates, rather than the crossed cylinder²⁻⁴ or sphere-on-flat geometries⁵ that have been so useful for nanometer-scale force measurements, was not only to explore flow at these intermediate length scales, but also to produce a contact area large enough for spectroscopic

characterization of the resulting molecular structure and orientation. Examples of plates that we have used include polished quartz and silicon with diameters up to several centimeters (as discussed below).

The principal restrictions on the minimal plate separation are surface roughness and ambient dust. In our experience to date, airborne dust limits this experiment to plate separations not less than ca. $3 \mu\text{m}$. Airborne dust particles are a problem at present because at present this apparatus is housed in ordinary laboratory air. In the absence of dust, surface roughness limits it to plate separations not less than ca. $0.1 \mu\text{m}$. For economic reasons, we have largely limited the plate separations to values $>3 \mu\text{m}$ for the practical reason that we are leery of scratching expensive finely polished glass plates. In future work, we hope that all of these difficulties may be side-stepped by employing curved cylindrical lenses with large radius of curvature, on the order of 1 m.

A schematic diagram of the device is given in Fig. 1. The device has four main functions, discussed below.

II. ACHIEVEMENT AND CHARACTERIZATION OF PARALLEL ALIGNMENT AT CONTROLLED SEPARATIONS

Top and bottom plates are mounted on three finely polished alignment rods whose ends are anchored at a solid metal support such that the rods are parallel to close tolerance. The top sample plate is mounted on a support that is clamped to these rods. The bottom sample plate is mounted to a support that rides up and down the rods on precision axial ball bearings. The bearings provide a coarse level of plate alignment as shown in Fig. 1.

To provide more accurate parallel alignment than this, and also to provide fine control of separation, the main idea is to push against the bottom surface at three tripod legs by the action of inchworms. Inchworms, rather than some other piezoelectric device, were chosen because of their negligible dimensional drift in the rest state. The inchworms that we use (Burleigh Instruments) possess a travel distance of 6.5 mm and a step resolution of 4 \AA .

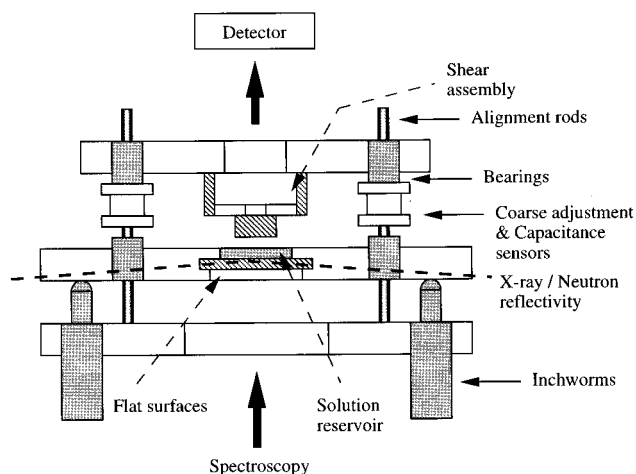


FIG. 1. Schematic diagram showing the four functions of the micron-gap rheo-optics device. (i) Capacity to position smooth plates to be parallel at controlled separations from ~ 0.1 to $500 \mu\text{m}$. Coarse positioning is produced by three alignment rods. Fine adjustments of the tilt and separation are accomplished by inchworm devices positioned as a tripod. In the diagram, the third inchworm and third alignment rod are not shown for clarity. The inchworms have a travel of 6.5 mm and distance control of 4 \AA . (ii) The plate-plate separation is measured either by interferometry or by capacitance sensors positioned near the three alignment rods (one is not shown for clarity). (iii) To implement shear measurements, the top surface hangs from two piezoelectric bimorphs attached to a solid support. A sinusoidally periodic voltage (i.e., force) is applied to one bimorph (the “sender” bimorph); this produces deflection in the bimorph and the top surface slides relative to the bottom one. The resulting amplitude and phase of displacement are detected at a symmetrically placed “receiver” piezoelectric bimorph. (iv) Spectroscopic characterization of the confined film, either during shear or in the quiescent state, is possible in various ways. Infrared and dielectric characterization are indicated by the arrows directed from the bottom to the top of the figure. X-ray and neutron beams can also be directed in this direction, but a reflection geometry, as indicated in the figure, is also possible.

To determine the tilt and separation between the plates, interferometric or capacitance methods can be used. Interferometry can be performed with visible light or in the infrared. The equations to relate wavelengths of constructive interference to surface separation are well known.^{6,7} Alternatively, capacitance is used to infer the plate-plate separation from textbook equations. For a typical area of 3 cm^2 , the capacitance in air is on the order of 25 pF at $D=35 \mu\text{m}$. The excellent agreement between surface separation measured by interferometry and by capacitance is illustrated in Fig. 2.

To illustrate the parallel alignment that can be achieved, we first consider data acquired by white light interferometry. White light was directed through polished quartz lenses (Melles-Griot, $\lambda/10$) that had been sputter-coated with 600 \AA of silver. The light that emerged was imaged by an optical microscope, dispersed by a $1/2 \text{ m}$ spectrometer, and recorded by a charge-coupled-device (CCD) camera. To the extent that the opposed plates are parallel, fringes of constructive interference should appear at a fixed wavelength regardless of spatial position on the plate. In Fig. 3, linear spatial position is plotted against wavelength of constructive interference. The vertical lines indicate parallel alignment in this direction. Quantitative analysis of the tilt of fringes in Fig. 3 shows a tilt of $6 \times 10^{-6} \text{ rad}$ (0.0003°).

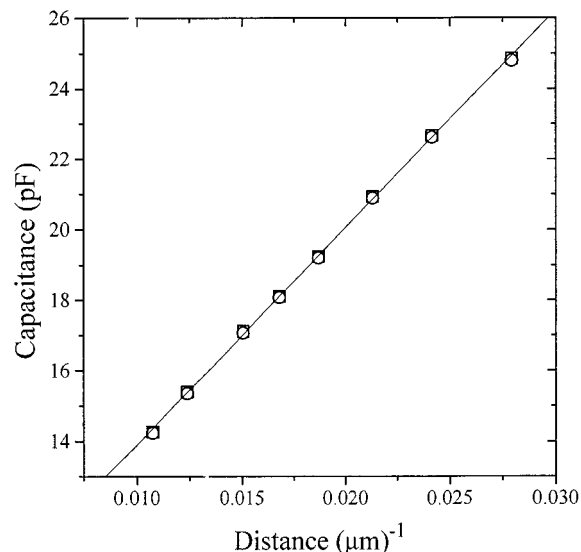


FIG. 2. Comparison of surface-surface separation measured by capacitance (circles) and conventional multiple beam interferometry between silver-coated quartz lenses separated by air (squares). Textbook equations for a capacitor and for multiple beam interferometry were used to infer the surface-surface separation. Note that an extrapolation to infinite thickness ($1/D=0$) is unwarranted because the calibration of our capacitor bridge would be nonlinear over such a large thickness range.

These measurements probed a one-dimensional cross section of one small area of the plate-plate contact. To check other positions, the incident white light source was directed onto other regions of the plate. To check a cross section of any region in an orthogonal direction, a dovetail prism rather than a normal 90° prism was used to observe the interference fringes.

The sharpness of such fringes provides additional information. In the bottom panel of Fig. 2 we plot the intensity of these fringes (top panel) against wavelength. From the width of the peaks we estimate the finesse, $\Delta\nu/\Delta\nu_s \sim 5$ ($\Delta\nu$ is the full width at half height and $\Delta\nu_s$ is the fringe separation). This gives the surface roughness, equivalent to $\lambda/5$ (λ is the incident wavelength).

For opaque samples, optical interferometry is not possible; we then measure capacitance to infer the plate-plate separation. The following iterative scheme is employed. First, the absolute plate separation is measured. This can be done either from capacitance between the plates or, for silicon and germanium plates, by infrared interferometry using a commercial Fourier transform infrared spectrometer (FTIR) detector. But interferometry with an FTIR detector lacks spatial resolution of the kind shown in Fig. 3. In this case, to characterize the plate tilt, we analyze capacitance changes at three capacitance sensors mounted on the three alignment rods shown in Fig. 1. The absolute capacitance at these sensors is not of interest (they are spaced, without being precise about it, at separations on the order of $100 \mu\text{m}$). Instead, we focus upon relative changes of capacitance when we play with the relative plate-plate tilt.

Small changes of tilt are produced deliberately by translating, in turn, each of the three inchworm positioning de-

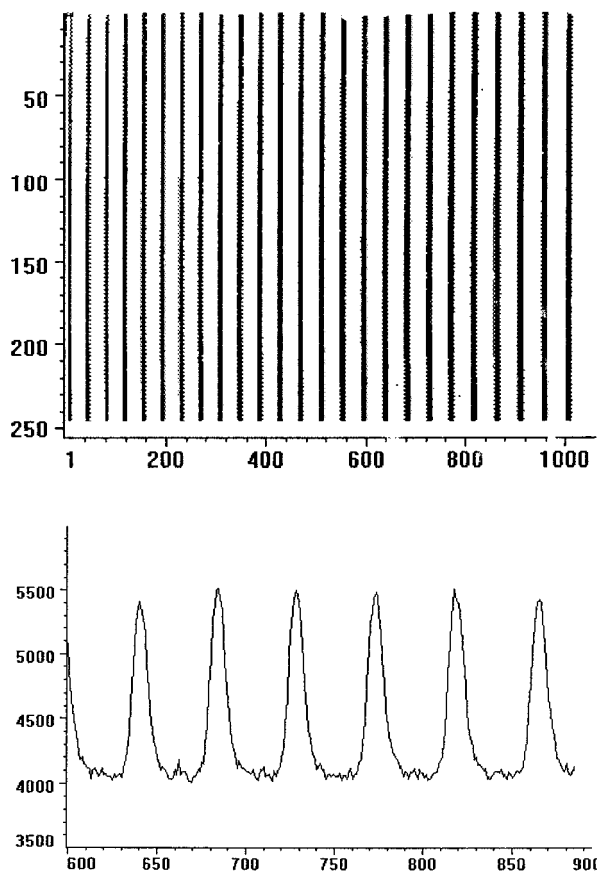


FIG. 3. Illustration of parallel alignment. (Top panel). White-light interferogram measured using a CCD camera attached to a 1/2 m spectrometer. Vertical lines show fringes of constructive interference when white light was directed through silvered plates. If the plates had not been parallel, deviations from vertical fringes would have been observed, since the surface-surface separation would then have depended on the lateral position along the plates. In this graph, units of the x and y axes are pixels. The y axis had lateral resolution of $6.25 \mu\text{m}$ per pixel. The x axis had wavelength resolution of 0.8370 \AA per pixel. In this example, the plates were separated by a polydimethylsiloxane (PDMS) fluid with refractive index 1.4040, indicating that the surface-surface separation was $32.22 \mu\text{m}$. The resolution of surface-surface separation was $0.009 \mu\text{m}$ at this separation and improved dramatically as the separation was reduced. Tilt between the opposed surfaces, measured from tilt of fringes in the graph, corresponds to a tilt of 6×10^{-6} rad (0.0003°). (Bottom Panel). Plot of the intensity of the white-light interferogram shown in the Top Panel (y axis, arbitrary units) against wavelength (units of \AA). From the width of these Fabry-Perot fringes we estimate the finesse, $\Delta\nu/\Delta\nu_s \sim 5$. This implies surface roughness of $\lambda/5$ (see text for explanation of symbols).

vices shown in Fig. 1. The resulting changes of capacitance at the sensor positions are observed. When the bottom plate is tilted in this fashion from three different legs, the angle of tilt is found by identifying the leg from which tilt produces the largest change of capacitance. It is then a straightforward exercise to adjust the inchworm positions, and therefore the tilt angle, to produce parallel alignment. The tedium of this exercise makes computer automatization useful. The signature of parallel alignment is that translating all three inchworms by the same vertical distance produces the same change of plate-plate separation.

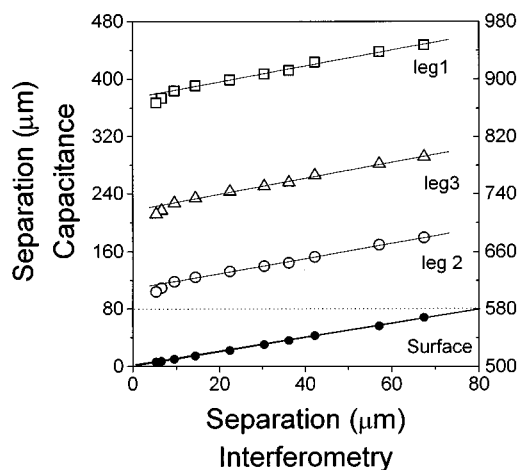


FIG. 4. Comparison of plate-plate separation measured by capacitance and conventional multiple beam interferometry. The sample was two silvered quartz lenses separated by air. Capacitance readings at four points are plotted against plate-plate separation measured by optical interferometry. The line labeled “surface” shows the numerical agreement between separations determined by capacitance and by white-light interferometry. The lines labeled “Leg 1,” “Leg 2,” and “Leg 3” show that the same resolution is obtained when capacitance is measured at the tripod legs described above. Note that the closer the surface-surface separation, the higher was the accuracy of capacitance measurement.

III. COMPARISON OF CAPACITANCE AND INTERFEROMETRIC MEASUREMENTS OF SURFACE-SURFACE SPACING

An example of parallel alignment determined by capacitance is shown in Fig. 4. Capacitance readings at 4 points are plotted against plate-plate separation measured by optical interferometry. The line labeled “surface” shows the numerical agreement between separations determined by capacitance and by white-light interferometry. The lines labeled “Leg 1,” “Leg 2,” and “Leg 3” show that the same resolution is obtained when capacitance is measured at the tripod legs described above. However, a key point is that the closer the surface-surface separation, the higher the accuracy of capacitance measurement.

IV. SHEAR RHEOLOGY

For shear rheology at these spacings, we adapt piezoelectric methods developed previously.^{2,3,8} Briefly, the top surface hangs from two piezoelectric bimorphs attached to a solid support. A sinusoidally periodic voltage (i.e., force) is applied to one bimorph (the “sender” bimorph); this produces deflection in the bimorph and the top surface slides relative to the bottom one. The resulting motion is sensed from voltage induced in a symmetrically placed second bimorph (the “receiver”). By comparing the amplitude and phase of this signal with that measured by calibrating the shear device in the absence of sample,^{2,3,8} the in-phase and out-of-phase components of the viscoelastic response are measured. The amplitude and phase are detected by a lock-in amplifier or spectrum analyzer. A typical frequency range is 0.1–700 Hz, with shear displacement amplitude $0.1\text{--}10 \mu\text{m}$.

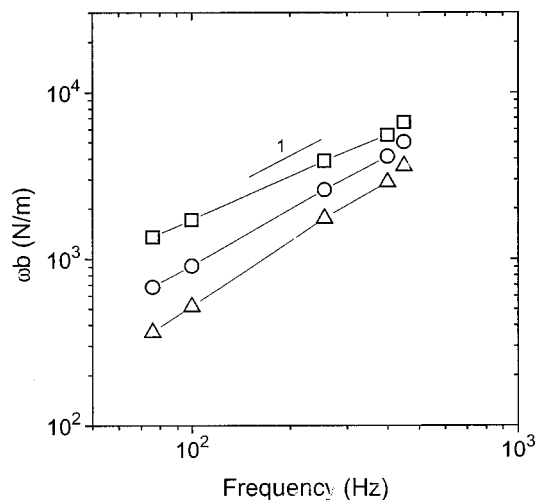


FIG. 5. Log-log plot of the viscous force constant for PDMS oil (970 cP), plotted versus frequency at three surface-surface separations: 30.25, 41.22, and 53.28 μm (squares, circles, and triangles, respectively). Here ω denotes radian frequency. The slope on the log-log plot, for frequency-independent viscosity, would be unity. The data at each of these thicknesses agrees with the known viscosity within the experimental uncertainty; small deviations from unity in this log-log graph are attributed to a humid environment. The performance of this device will be improved by isolating the piezoelectric bimorphs from the ambient atmosphere.

Unless one is close to resonance, force constants out-of-phase and in-phase with the drive (k and ωb , respectively) are determined as

$$\omega b = k_s [(A_0/A) \sin \theta], \quad (1)$$

$$k = k_s [(A_0/A) \cos \theta - 1]. \quad (2)$$

Here A_0 is the calibrated output amplitude when the surfaces are separated in gas atmosphere and A is the measured value in the presence of the sample confined liquid. The angle θ is the phase difference between the calibration sinusoidal waveform and that in the presence of liquid. The parameter k_s is an elastic constant of the apparatus.

Figure 5 shows a log-log plot of the viscous force constant ωb measured as a function of frequency for a sample whose known viscosity is specified in the figure caption. The data demonstrate the potential of this device. The scatter of data in Fig. 5 is believed to reflect drifts of piezoelectric circuitry in the ambient laboratory air, whose humidity drifts with time. Our previous measurements that used this approach were performed inside a sealed chamber with strict control of the humidity.^{2,3,8} For this new device, isolation of the piezoelectric bimorphs from the laboratory environment is underway.

In summary, we have shown how to prepare parallel plates at controlled separations without fundamental limitation, other than surface roughness, of the type of surface that can be employed. We speculate that this apparatus will be useful in conjunction with ancillary dielectric or infrared characterization in the direction normal to the plates, and x -ray and neutron reflectivity.

ACKNOWLEDGMENTS

We are indebted to Iwao Soga and Yoon-Kyoung Cho for numerous discussions and for the measurements shown in Fig. 4. This work was supported by generous donations from the Exxon Research and Engineering Corp., and by grants from the Air Force Office of Scientific Research and the National Science Foundation (Tribology Program).

¹J. D. Ferry, *Viscoelastic Properties of Polymers*, 3rd ed. (Wiley, New York, 1980).

²J. Van Alsten and S. Granick, *Phys. Rev. Lett.* **61**, 2570 (1988).

³J. Peachey, J. Van Alsten, and S. Granick, *Rev. Sci. Instrum.* **62**, 463 (1991).

⁴J. N. Israelachvili, P. M. McGuigan, and A. M. Homola, *Science* **240**, 189 (1988).

⁵A. Tonck, D. Mazuyer, and J. M. Georges (unpublished).

⁶S. C. Hunter and F. R. N. Nabarro, *Philos. Mag.* **43**, 538 (1952).

⁷J. N. Israelachvili, *J. Coll. Interface Sci.* **44**, 259 (1973).

⁸H.-W. Hu and S. Granick, *Langmuir* **10**, 3857 (1994).